NAM

Updated Empirical GMPEs for PGV from Groningen Earthquakes – March 2019

Julian J Bommer, Peter J Stafford & Michail Ntinalexis

Datum March 2019

Editors Jan van Elk & Dirk Doornhof

General Introduction

The hazard from induced earthquakes is primarily presented by the ground motion to which buildings and people are subjected. The prediction of ground motion, resulting from the earthquakes in the Groningen area induced by the production of gas, is critical for the assessment and prognosis of building damage and personal risk.

The research into the development of the ground motion prediction methodology started in 2012 and continues as more ground motion data from Groningen earthquakes is collected. The prime goal of these studies has been the assessment of ground motion for risk assessment. This means the focus has primarily been on the prediction of ground acceleration for larger events, extrapolating from the currently available data obtained from earthquakes with magnitude below M=3.6 to earthquakes with magnitude in the range from M=4 to M=5 and up to M_{max} (Ref. 1). The development of these Ground Motion Prediction Models for the assessment of risk has been documented in several reports (Ref. 2, 3, 4, 5 and 6). The model used in the current hazard and risk assessment is GMM version 5 (Ref. 6).

Additionally, a Ground Motion prediction methodology was developed for smaller earthquakes within the range of current experience. This empirical methodology was developed for operational use within the context of building damage. The Ground Motion Model developed in 2016 aimed to accurately predict ground motion for earthquakes in the same range as the historical data base, primarily from M=2.5 to M=3.6 (Ref. 9). In addition to the peak ground acceleration this methodology also covers peak ground velocity and V_{top}. These last two metrics of ground motion are especially relevant for building damage and comparison with the Guidelines of the SBR (Stichting Bouw Research) (Ref. 7 and 8).

During 2017, the requirement for prediction of ground motions for earthquakes smaller than M=2.5 was identified. The empirical methodology was therefore extended to cover the range of earthquakes with magnitude in the range from M=1.8 to M=3.6 (Ref. 10).

This current update of the empirical ground motion prediction methodology also includes the earthquakes during 2018, most notably the Zeerijp earthquake (of 8th January 2018) and the Garsthuizen earthquake (13 April 2018), and the recent recalibration of the accelerometers located at the G-stations of the KNMI seismic monitoring network.

References:

1. Report on Mmax Expert Workshop, Mmax panel chairman Kevin Coppersmith, June 2016
2. Technical Addendum to the Winningsplan Groningen 2013; Subsidence, Induced Earthquakes and Seismic Hazard Analysis in the Groningen Field, Nederlandse Aardolie Maatschappij BV (Jan van Elk and Dirk Doornhof, eds), November 2013.
3. Development of Version 1 GMPEs for Response Spectral Accelerations and for Strong-Motion Durations, Julian J Bommer, Peter J Stafford, Benjamin Edwards, Michail Ntinalexis, Bernard Dost and Dirk Kraaijpoel, March 2015.
4. Development of Version 2 GMPEs for Response Spectral Accelerations and Significant Durations for Induced Earthquakes in the Groningen field, Julian J Bommer, Bernard Dost, Benjamin Edwards, Adrian Rodriguez-Marek, Pauline P Kruiver, Piet Meijers, Michail Ntinalexis & Peter J Stafford, October 2015
5. V4 Ground-motion Model (GMM) for Response Spectral Accelerations, Peak Ground Velocity and Significant Duration in the Groningen field, Julian Bommer, Bernard Dost, Benjamin Edwards, Pauline Kruiver, Pier Meijers, Michail Ntinalexis, Adrian Rodriguez-Marek, Elmer Ruigrok, Jesper Spetzler and Peter Stafford, Independent Consultants, Deltares and KNMI, June 2017 with Parameter files - V4 Ground-Motion Model (GMM) for Response Spectral Accelerations, Peak Ground Velocity, and Significant Durations in the Groningen Field, Supplement to V4 GMM, Julian Bommer and Peter Stafford, Independent Consultants, June 2017
6. V5 Ground-Motion Model for the Groningen Field, J.J. Bommer, B. Edwards, P.P. Kruiver, A. Rodriguez-Marek, P.J. Stafford, B. Dost, M. Ntinalexis, E. Ruigrok, J. Spetzler, 30th October 2017.
7. Meet- en beoordelingsrichtlijn: Trillingen - Deel B Hinder voor personen, Stichting Bouw Research, 2006.
8. Meet- en beoordelingsrichtlijn: Trillingen - Deel A Schade aan gebouwen, Stichting Bouw Research, 2010.
9. Empirical Ground-Motion Prediction Equations for Peak Ground Velocity from Small-Magnitude Earthquakes in the Groningen Field Using Multiple Definitions of the Horizontal Component of Motion, Julian J Bommer, Peter J Stafford & Michail Ntinalexis, November 2016
10. Empirical Ground-Motion Prediction Equations for Peak Ground Velocity from Small-Magnitude Earthquakes in the Groningen Field Using Multiple Definitions of the Horizontal Component of Motion, Updated Model for Application to Smaller Earthquakes, Julian J Bommer, Peter J Stafford & Michail Ntinalexis, November 2017

These reports are also available at the study reports page of the website www.namplatform.nl.

NAM

Title	**Updated Empirical GMPEs for PGV from Groningen Earthquakes – March 2019**		**Date**	March 2019
			Initiator	NAM
Autor(s)	Julian J Bommer, Peter J Stafford & Michail Ntinalexis	**Editors**	Jan van Elk & Dirk Doornhof	
Organisation	Researcher primarily from Imperial College, London.	**Organisation**	NAM	
Place in the Study and Data Acquisition Plan	Study Theme: Ground Motion Prediction Comment: The prediction of Ground Motion is central to the hazard assessment. This report describes a Ground Motion Prediction methodology for operational use in the damage protocol, covering the magnitude range from M=1.8 to M=3.6. This current update of the empirical ground motion prediction methodology also includes the earthquakes during 2018, most notably the Zeerijp earthquake (of 8th January 2018) and the Garsthuizen earthquake (13 April 2018), and the recent recalibration of the accelerometers located at the G-stations of the KNMI seismic monitoring network.			
Directliy linked research	(1) Hazard Assessment. (2) Building Damage (DS1).			
Used data	Accelerograms from the accelerometers placed in the Groningen field. Description of the shallow geology of Groningen.			
Associated organisation	Imperial College (London).			
Assurance	Internal to the Hazard Team.			

Updated Empirical GMPEs for PGV from Groningen Earthquakes

Julian J Bommer, Peter J Stafford & Michail Ntinalexis

A report to NAM

Revision 1

4 March 2019

Table of Contents

1. Introduction and Scope

As part of its response to induced earthquakes in the Groningen gas field, NAM has for several years been developing and refining models for the estimation of seismic hazard and risk. An essential component of the hazard and risk estimations is a model for the prediction of ground-motion amplitudes and durations at the ground surface as a result of all potential induced and triggered earthquakes (*e.g*., Bommer *et al*., 2017a; Bommer *et al*., 2017b).

In parallel to the ground-motion model (GMM) for spectral accelerations and durations that is applicable for moderate-to-large magnitude earthquakes, an empirical model for the prediction of peak ground velocity (PGV) was developed for applications related to tolerable shaking levels (Bommer *et al*., 2017c). This brief report presents an update of the model that has been made due to the acquisition of additional ground-motion recordings in the field and also some calibration corrections to surface accelerographs of the G-network operated by KNMI. As before, equations are derived for three different definitions of the horizontal component of motion based on different treatments of the horizontal components from each accelerogram: the geometric mean, the larger of the two, and the peak corresponding to the maximum value obtained by rotating the recorded components.

Section 2 of the report presents the expanded database used to derive the new model. The derivation of the new model is presented in Section 3 of the report, which also includes comparisons with the previous model from November 2017. The report ends with a brief discussion of the new model in Section 4.

2. Ground-Motion Database

The database used to derive the previous version of the model contained 1,014 recordings from 47 earthquakes with magnitudes ranging from M_L 1.8 to 3.6. In the updated database there are only an additional 8 earthquakes (with magnitudes ranging from M_L 1.8 to 3.4) but these additional earthquakes contribute 693 new recordings. The location of the new earthquakes is shown in Figure 2.1, together with the epicentres of the events in the database used to derive the 2017 model. The fact that a 17% increase in the number of events in the database is accompanied by a 68% increase in the number of recordings is very clear testimony to the value of the expanded networks that are now operational in the Groningen field.

Figure 2.2 shows the magnitude-distance distribution of the expanded database. While it can be seen that the additional earthquakes have contributed data in the higher magnitude ranges (and also extended the maximum distance at which such events have been recorded), it is also the case that there has been a much larger increase in the number of recordings from smaller events: three-quarters of the additional

recordings are from earthquakes with magnitudes of $M_L \leq 2.2$. Whereas the database previously showed a reasonably uniform distribution with respect to magnitude and distance, it is now arguably biased towards smaller magnitudes, which is consistent with the more frequent occurrence of smaller events. The regression techniques used to fit the equations to the data account for the distribution of the data in order to avoid biased estimates, hence in itself the greater number of small-magnitude recordings is not necessarily a problem.

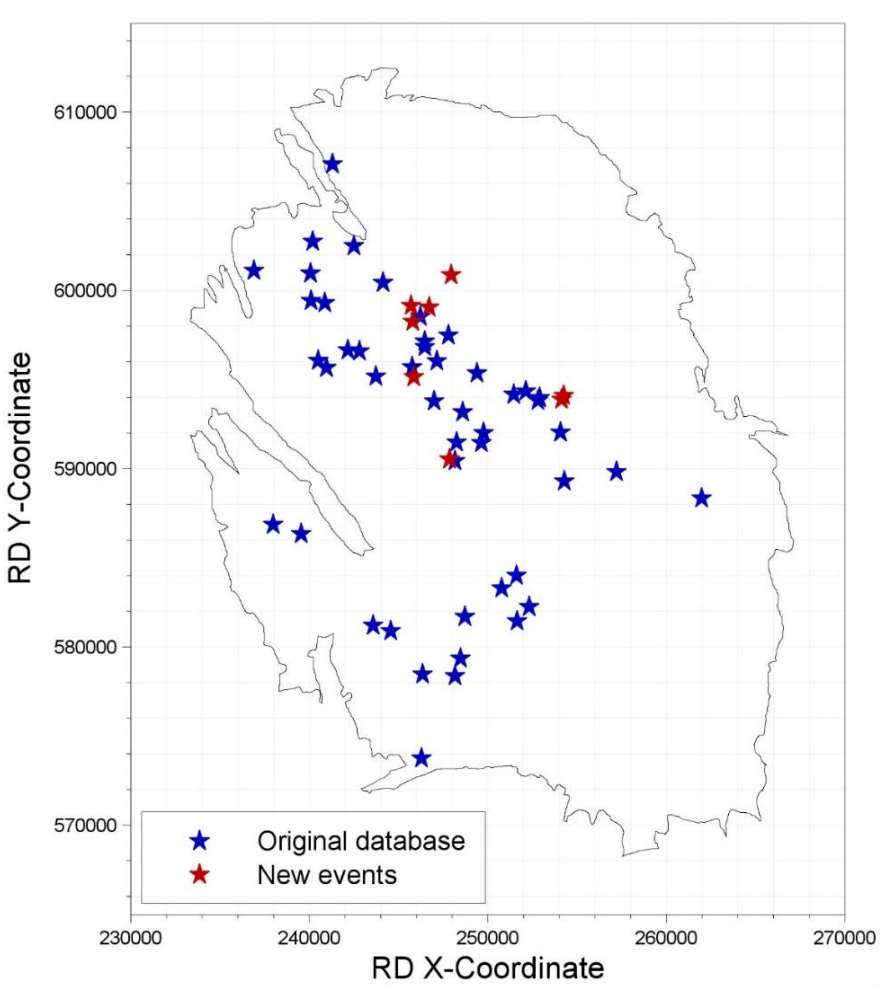

Figure 2.1. Map of the Groningen field; earthquake epicentres are shown in stars, with red symbols corresponding to the new additions to the database.

Table 2.1 lists all of the earthquakes in the database together their main metadata: the local magnitude, epicentral coordinates, date and time of occurrence, and the number of useable recordings obtained from the accelerograph networks. With regard to the first column in Table 2.1, the following ID coding was used: standard numbers are used for earthquakes of $M_L \geq 2.5$, the prefix A is used for earthquakes that occurred in 2013 and 2014, before the G-network was online, the prefix B is used for 2015, when a part of the G-network was online, and C is used for earthquakes including and after

2016, when most, and almost all, of the G-network has been online. The new prefix D corresponds to events of magnitude ML < 2.5 that have occurred since the beginning of 2018. The new events are added to their respective groups and highlighted for ease of identification. Also worthy of note is that following the calibration correction, 17 records from the 47 earthquakes already in the database were brought into the analyses, leading to a total of 1,724 records from 55 earthquakes in the final dataset.

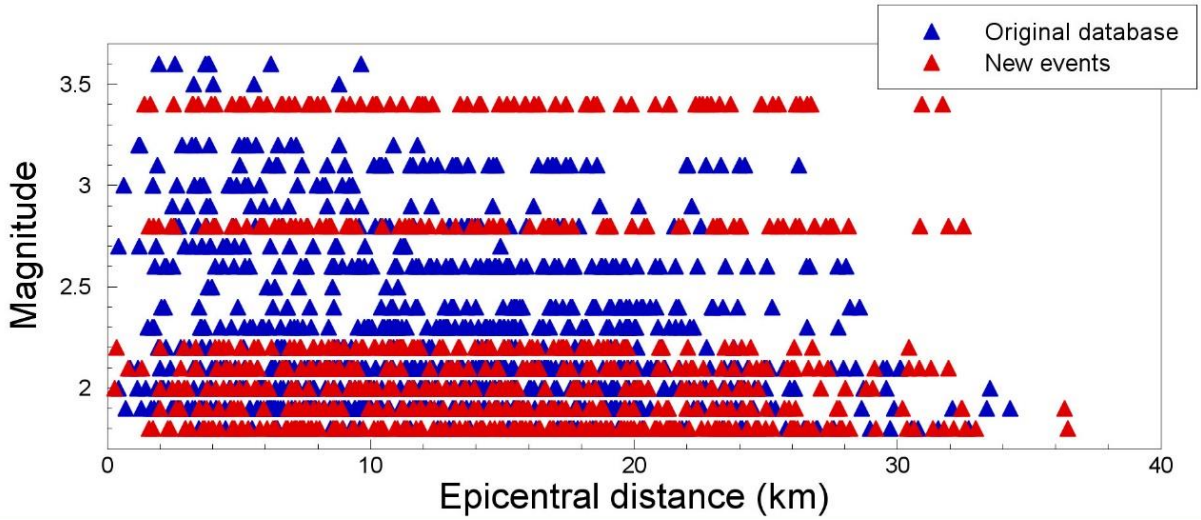

Figure 2.2. Magnitude-distance distribution of the database used to derive the new equations, with red symbols corresponding to the new additions.

The largest recorded value of PGV on any single component within the expanded database is still 3.46 cm/s, which was on the NS component of the MID1 recording obtained at 2 km from the epicentre of the 2012 Huizinge M_L 3.6 earthquake. The second highest value of PGV is now 3.21 cm/s, which was recorded at the BGAR station during the M_L 3.4 Zeerijp earthquake of 8 January 2018, one of the new additions to the database. Together, the 2012 Huizinge and 2018 Zeerijp earthquakes contribute all of the seven highest PGV recordings. The amplitudes overall, however, remain quite low: only 21 records have a PGV of at least 1 cm/s (previously there were 14, several of the additional records coming from the Zeerijp event), which represents just over 1% of the database. About one-eighth of the total number of records have a component with PGV ≥ 0.1 cm/s and for about one-half of the data the larger component of PGV does not reach 0.01 cm/s.

In terms of the maximum rotated component—which is assumed to be closest to the V_{TOP} definition—a total of 160 records (9.3% of the data) exceed the 1.5 mm/s threshold. Just 22 of these recordings are from events of magnitude M_L < 2.5, and these are all from epicentral distances of less than 4 km. Only for magnitudes M_L > 3 is this level of motion exceeded by any record obtained at more than 10 km from the epicentre.

Table 2.1. List and basic metadata of earthquakes included in the extended database; the 8 highlighted events are those added since the 2017 version of the model was derived

EQ ID	M	RD-X	RD-Y	No. Records	Date & Time
01	3.5	242159	596659	4	2006-08-08-05:04:00
02	2.5	242826	596579	1	2006-08-08-09:49:23
03	3.2	243740	595168	6	2008-10-30-05:54:29
04	2.6	240955	595673	3	2009-04-14-21:05:25
05	3	246479	597129	5	2009-05-08-05:23:11
06	2.5	242496	602509	5	2010-08-14-07:43:20
07	3.2	248253	591487	8	2011-06-27-15:48:09
08	2.5	241305	607070	3	2011-08-31-06:23:57
09	2.5	249399	595368	1	2011-09-06-21:48:10
10	3.6	240504	596073	7	2012-08-16-20:30:33
11	2.7	240112	599405	3	2013-02-07-22:31:58
12	3.2	240085	600945	3	2013-02-07-23:19:08
13	2.7	246230	598516	2	2013-02-09-05:26:10
14	3	248163	590446	2	2013-07-02-23:03:55
15	2.8	247166	596048	5	2013-09-04-01:33:32
16	3	247804	597489	14	2014-02-13-02:13:14
17	2.6	248489	579359	5	2014-09-01-07:17:42
18	2.8	239565	586336	12	2014-09-30-11:42:03
19	2.9	240890	599307	18	2014-11-05-01:12:34
20	2.8	244561	580898	19	2014-12-30-02:37:36
21	2.7	246987	593800	19	2015-01-06-06:55:28
22	3.1	251603	584016	42	2015-09-30-18:05:37
23	2.6	251654	581456	71	2017-05-27-15:29:00
24	3.4	245790	598262	79	2018-01-08-14:00:52
25	2.8	245706	599151	85	2018-04-13-21:31:35
A0	1.9	244131	600435	2	2013-09-28-02:20:41
A1	1.9	248599	593173	2	2013-10-02-20:24:26
A2	2.0	252129	594346	11	2013-11-26-23:54:53
A3	2.3	250795	583309	10	2014-03-11-09:08:23
A4	1.9	254062	592047	9	2014-03-15-19:09:24
A5	2.1	236905	601108	10	2014-03-18-21:15:18
A6	2.1	248709	581699	9	2014-07-02-17:34:16
A7	2.0	251466	594165	9	2014-08-09-15:55:32
B0	1.9	246301	573749	31*	2015-02-12-16:05:53
B1	2.3	252916	593972	26	2015-02-25-10:02:56
B2	2.3	252806	593803	12	2015-03-24-13:27:56
B3	2.0	240203	602746	23	2015-05-27-10:52:10
B4	1.9	245771	595702	26	2015-06-06-23:39:15
B5	2.1	237996	586878	32*	2015-07-07-03:09:00
B6	2.0	246365	578459	30*	2015-08-18-07:06:12
B7	2.3	257224	589809	50*	2015-10-30-18:49:01
C0	2.4	248172	578382	58	2016-02-25-22:26:30
C1	2.1	252307	582249	56*	2016-09-02-13:16:00
C2	1.9	249653	591435	51*	2016-11-01-00:12:28
C3	2.2	249776	591994	52	2016-11-01-00:57:46
C4	2.1	246483	596828	56	2017-03-11-12:52:48
C5	1.8	261993	588355	66*	2017-04-04-10:00:44
C6	2.0	243574	581189	70*	2017-04-26-13:56:49
C7	1.9	254299	589303	71*	2017-09-05-22:08:27
C8	1.8	247937	600864	87	2017-12-06-23:28:59
C9	2.1	246707	599059	87	2017-12-10-16:48:33
D0	2.0	245848	595146	90	2018-02-08-15:25:30
D1	2.2	247870	590510	90	2018-02-11-16:54:57
D2	1.9	254138	593864	88	2018-08-08-02:55:29
D3	1.8	254266	594089	87	2018-08-09-08:01:55

* Number of useable records increased following re-processing

3. Empirical Equations for PGV

The new equations have been derived in exactly the same way as the 2017 empirical models for PGV, as a simple function of local magnitude and epicentral distance. In previous studies, it was established that incorporation of the site classification through the parameter V_{S30} was found to exert a negligible influence hence the model is limited to the two fundamental explanatory variables of magnitude and distance.

3.1. Functional form and regressions

The extended database has not required any changes to the basic functional form used previously hence the equations have exactly the same structure. The equations are reproduced here so that the new model can be implemented without reference to previous reports. The basic equation for predicting PGV is:

$$\ln(PGV) = c_1 + c_2 M + g(R) \tag{3.1}$$

with PGV in cm/s, M being local magnitude, M_L, determined by KNMI and the distance term, R, is defined as in Eq.(3.2), which defines the magnitude-dependent near-source saturation of the attenuation curve:

$$R = \sqrt{R_{epi}^2 + [\exp(0.4233M - 0.6083)]^2} \tag{3.2}$$

The magnitude-dependent distance saturation term in Eq.(3.2) was obtained from regressions on Groningen recordings. The geometrical spreading term is segmented over three distances:

$$g(R) = c_4 \ln(R) \qquad R \le 6.32km \tag{3.3a}$$

$$g(R) = c_4 \ln(6.32) + c_{4a} \ln\left(\frac{R}{6.32}\right) \qquad 6.32 < R \le 11.62km \tag{3.3b}$$

$$g(R) = c_4 \ln(6.32) + c_{4a} \ln\left(\frac{11.62}{6.32}\right) + c_{4b} \ln\left(\frac{R}{11.62}\right) \qquad R > 11.62km \tag{3.3c}$$

Maximum likelihood regression was performed to find the coefficients of the functional form all three PGV definitions. The results are summarized in Table 3.1.

Table 3.1. Coefficients of Eqs. (3.1-3.3) for the prediction of PGV

Coefficient	PGV_{GM}	PGV_{Larger}	PGV_{MaxRot}
c_1	-5.59324	-5.20047	-5.07636
c_2	2.24816	2.28589	2.2835
c_4	-1.75493	-1.90988	-1.93283
c_{4a}	-1.14046	-1.11959	-1.10756
c_{4b}	-1.61257	-1.65679	-1.67393

3.2. Variability and event terms

The standard deviations of the residuals are an integral part of the equations, which predict probabilistic distributions of PGV rather than deterministic estimates of unique values. The total standard deviation, σ, is decomposed into a between-earthquake component, τ, and a within-earthquake component, ϕ; these are related as follows:

$$\sigma = \sqrt{\tau^2 + \phi^2} \tag{3.4}$$

The values of the standard deviations are reported in Table 3.2.

Table 3.2. Standard deviations of the PGV prediction models

Coefficient	PGV_{GM}	PGV_{Larger}	PGV_{MaxRot}
τ	0.25128	0.25169	0.25242
ϕ	0.48205	0.54001	0.53613
σ	0.54361	0.59578	0.59258

Figure 3.1 compares the variance components in Table 3.2 with those corresponding to the previous version of the model. The total random variability in the predictions, as represented by sigma, has been reduced compared to the previous model. The reduction is almost entirely due to a very substantial decrease in the inter-event (earthquake-to-earthquake) variability.

Figure 3.2 shows the event terms, which are listed in Table 3.3, plotted against magnitude, from which it can be appreciated that there are no discernible trends, which confirms that the model provides an unbiased fit to the data. Figure 3.3 shows the intra-event residuals against distance, which also confirms that the model is a good fit to the data. Trend lines fitted to these residuals have intercepts of 0.0007 or smaller, and gradients smaller than 0.00001, both of which are small enough to be considered negligible.

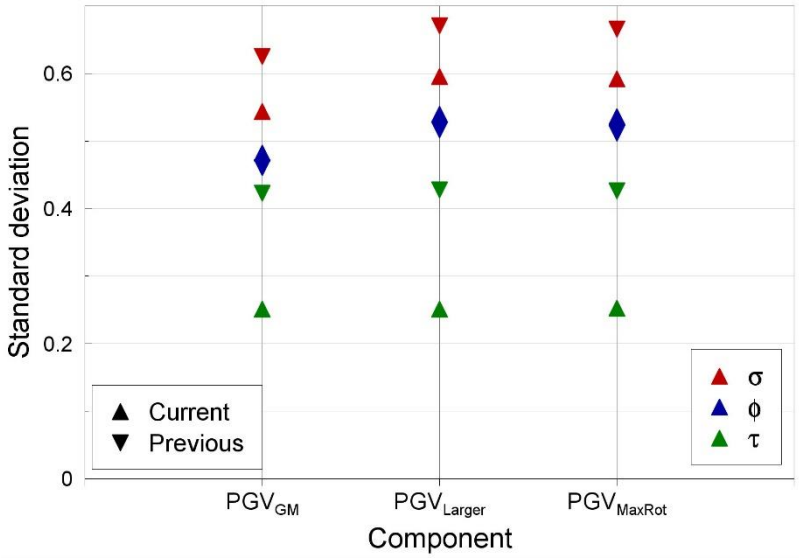

Figure 3.1. Comparison of variability associated with new model to the variance components of the November 2017 model

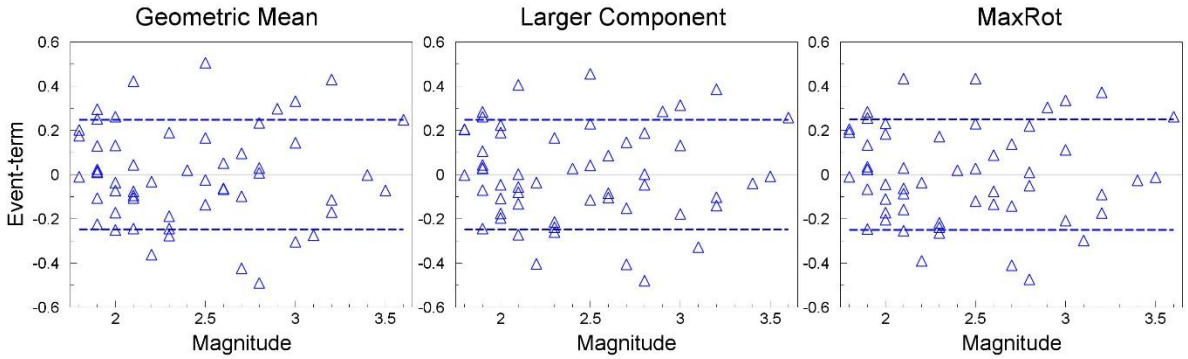

Figure 3.2. Event terms plotted against magnitude; the dashed lines represent one standard deviation of the inter-event variability.

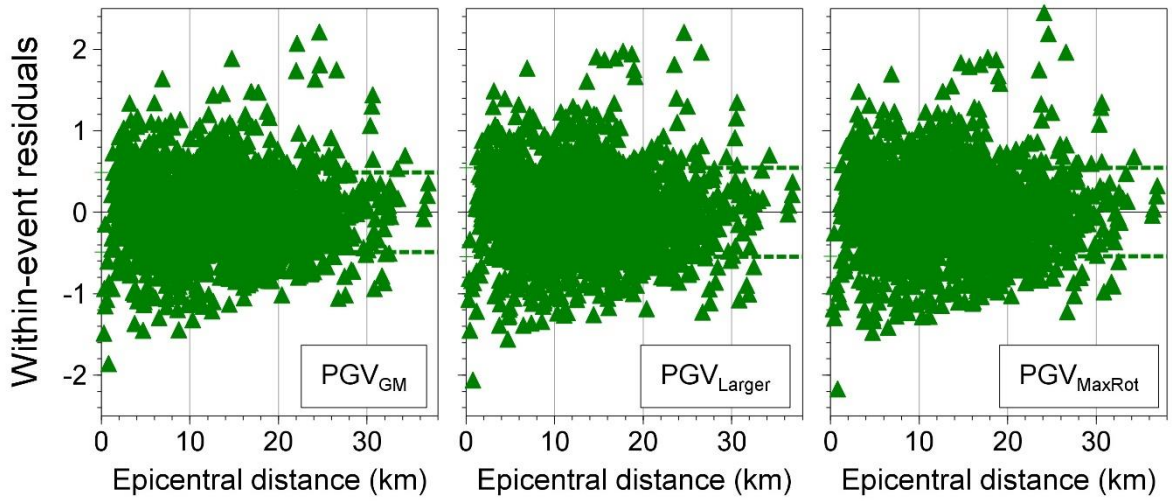

Figure 3.3. Intra-event residuals plotted against distance; the dashed lines represent one standard deviation of the intra-event variability.

Table 3.3. Event-terms for the PGV ground-motion model

EQ ID	M_L	PGV_{GM}	PGV_{Larger}	PGV_{MaxRot}
1	3.5	-0.0713	-0.0072	-0.0109
2	2.5	-0.0232	0.0428	0.0285
3	3.2	-0.1143	-0.1015	-0.0897
4	2.6	0.0524	0.0859	0.0883
5	3	-0.303	-0.1772	-0.2082
6	2.5	0.1671	0.2303	0.2298
7	3.2	0.4311	0.3857	0.3717
8	2.5	0.506	0.457	0.4339
9	2.5	-0.1363	-0.1147	-0.1197
10	3.6	0.2478	0.2587	0.2624
11	2.7	-0.0969	-0.1515	-0.141
12	3.2	-0.1693	-0.1391	-0.1737
13	2.7	0.0966	0.1471	0.1386
14	3	0.1443	0.133	0.1113
15	2.8	-0.4891	-0.4801	-0.474
16	3	0.3322	0.3139	0.3365
17	2.6	-0.0657	-0.1039	-0.1333
18	2.8	0.2338	0.1878	0.2199
19	2.9	0.2979	0.2865	0.3049
20	2.8	0.0299	-0.0449	-0.0493
21	2.7	-0.424	-0.4066	-0.4105
22	3.1	-0.2737	-0.3273	-0.2974
23	2.6	-0.0617	-0.0835	-0.0751
24	3.4	-0.0024	-0.0399	-0.0262
25	2.8	0.0091	0.0025	0.0097
A0	1.9	0.1303	0.1054	0.1332
A1	1.9	0.0242	0.0287	0.0249
A2	2	-0.2492	-0.1963	-0.2037
A3	2.3	-0.2759	-0.2607	-0.2645
A4	1.9	0.2512	0.2833	0.2849
A5	2.1	0.422	0.4066	0.4336
A6	2.1	-0.1065	-0.1319	-0.1575
A7	2	0.2623	0.2231	0.2312
B0	1.9	0.2969	0.2624	0.2568
B1	2.3	0.1896	0.1657	0.1726
B2	2.3	-0.2447	-0.214	-0.2372
B3	2	-0.0723	-0.1081	-0.1101
B4	1.9	-0.1068	-0.0699	-0.0662
B5	2.1	-0.0945	-0.0791	-0.0855
B6	2	0.1318	0.1905	0.185
B7	2.3	-0.1883	-0.2389	-0.2183
C0	2.4	0.0199	0.0274	0.0201
C1	2.1	-0.0751	-0.056	-0.0624
C2	1.9	0.015	0.0436	0.0358
C3	2.2	-0.0324	-0.0363	-0.0357
C4	2.1	0.0439	0.0029	0.0307
C5	1.8	0.2022	0.2049	0.1918
C6	2	-0.1709	-0.1763	-0.1719
C7	1.9	-0.2245	-0.2429	-0.2451
C8	1.8	-0.0105	-0.0019	-0.009
C9	2.1	-0.2444	-0.2715	-0.2548
D0	2	-0.0364	-0.0467	-0.0448
D1	2.2	-0.3613	-0.4035	-0.3908
D2	1.9	0.0109	0.0301	0.0241
D3	1.8	0.1763	0.2056	0.2065

3.3. Predictions of PGV

Figure 3.4 shows predicted median values of PGV from the three equations as a function of epicentral distance for three magnitudes that cover the likely range of application of these equations. The relative amplitudes obtained with the three different horizontal component definitions continue to be exactly as expected.

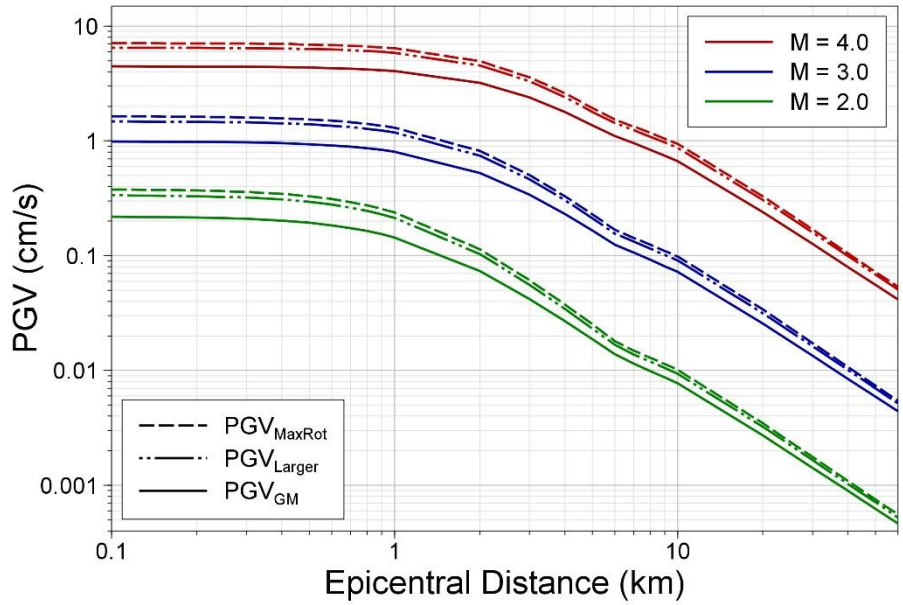

Figure 3.4. Predicted median PGV values against distance for three magnitudes

Figure 3.5 compares the median predicted PGV values from those obtained with the previous model, from which it can be appreciated that the differences are not particularly larger, especially at shorter distances. For small earthquakes, the median predictions have increased whereas at M_L 4.0—which corresponds to an extrapolation of the model beyond its strict limit of applicability—the near-source amplitudes have actually decreased a little. These observations essentially reflect a change in the magnitude scaling (Figure 3.6), which is most likely a result of the calibration issues, which affect only the G-network stations, impacting more on the smaller-magnitude events where records from that network dominate, whereas at larger magnitudes, recordings from the B-network still constitute a large proportion of the data. The magnitude scaling in the new model is less pronounced than in the previous model, such that the increase in PGV with each unit of magnitude is smaller than before. Figure 3.7 shows similar plots to those in Figure 3.5 except that instead of median predictions these are now the predictions at the 84-percentile level (*i.e.*, one standard deviation above the median). The differences at short distances are now reduced—except at M_L 4—as a result of the counter-balancing effects of higher medians and lower sigma values. The differences between the old and new models at distance are

also somewhat reduced, such that at this level the differences only become appreciable for PGV values below 1 mm/s.

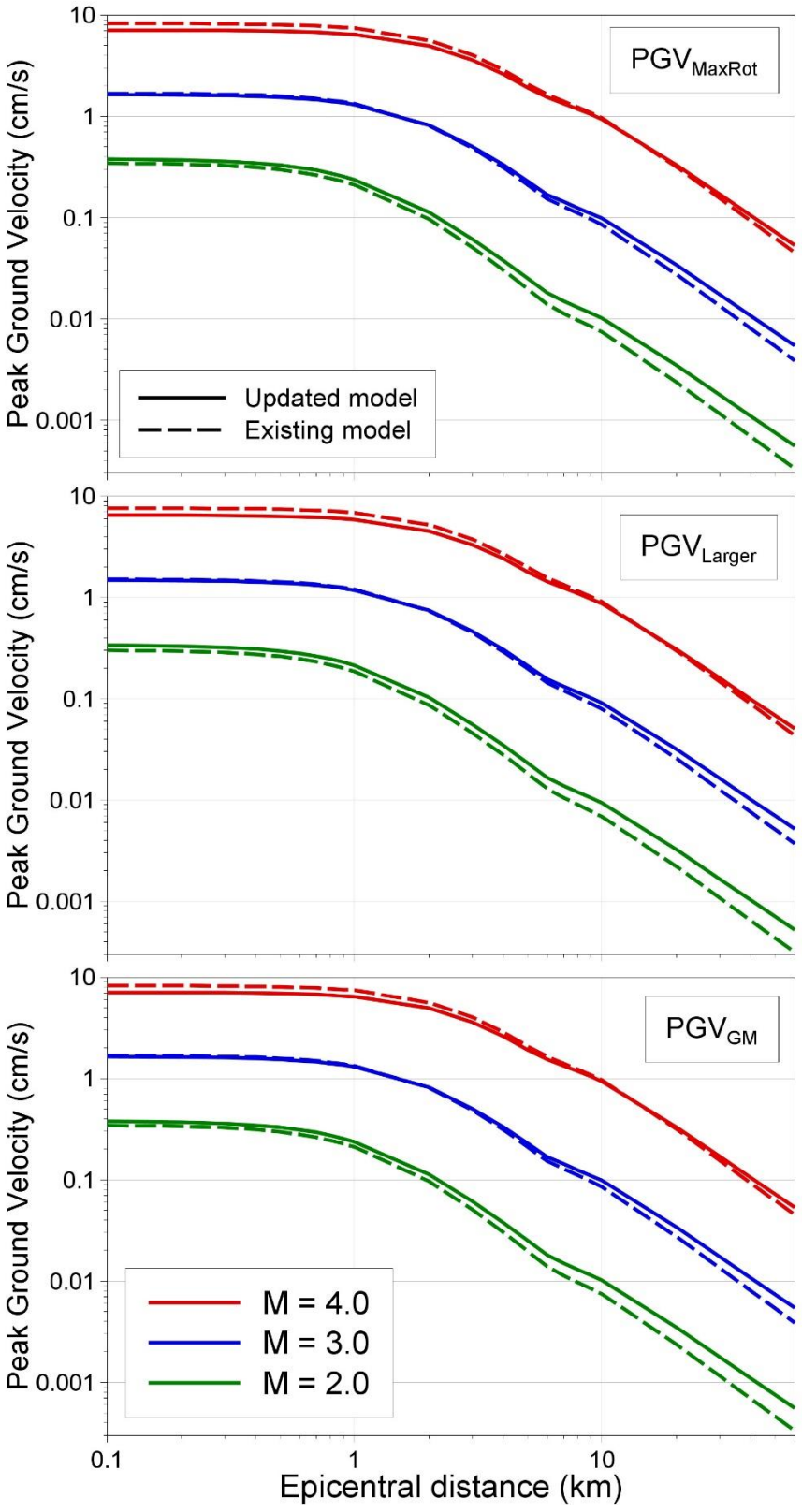

Figure 3.5. Predicted median PGV values from the old and new models against distance for magnitudes M_L 2, 3 and 4

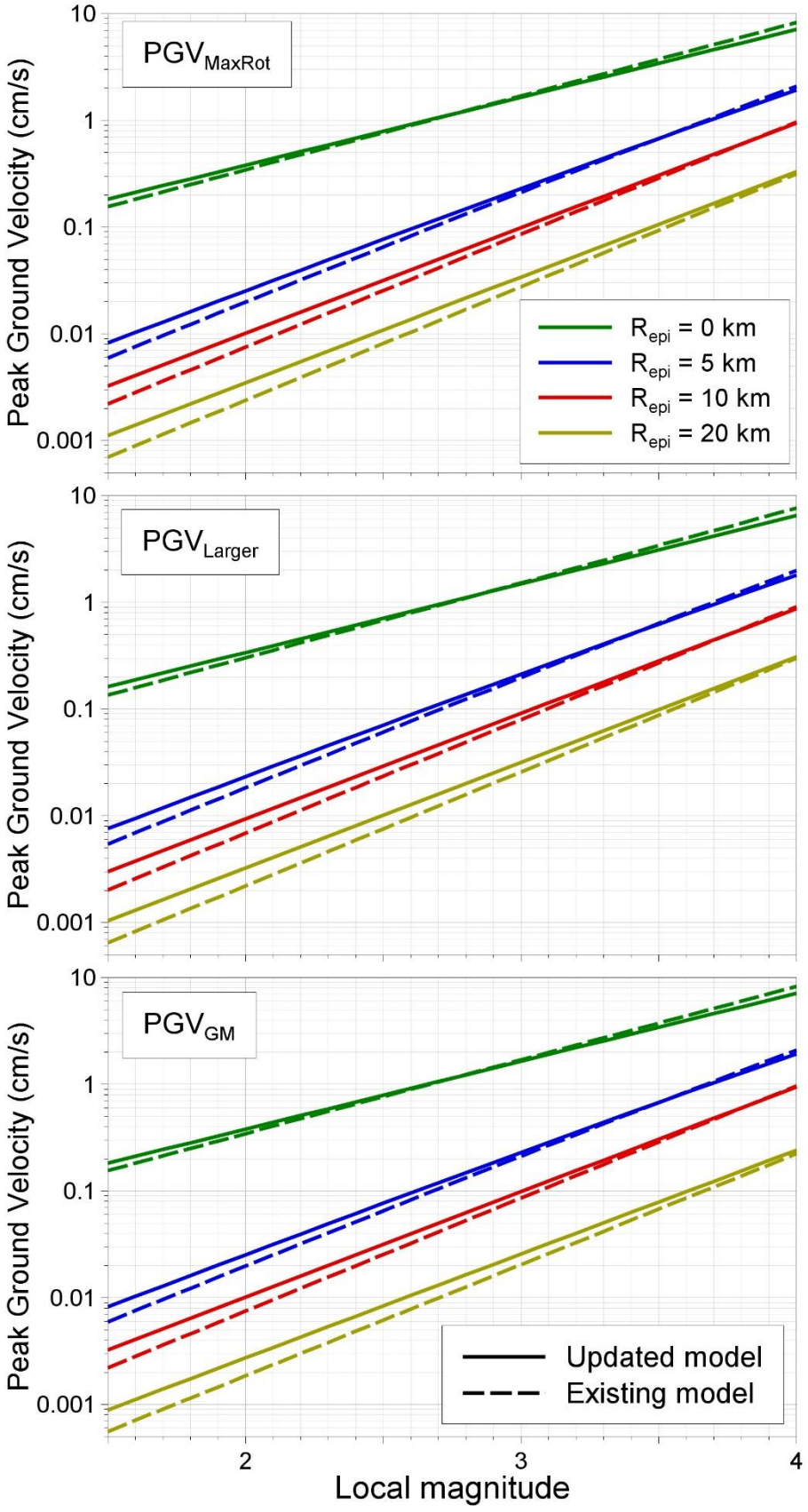

Figure 3.6. Predicted median PGV values from the old and new models against magnitude at four different values of epicentral distance

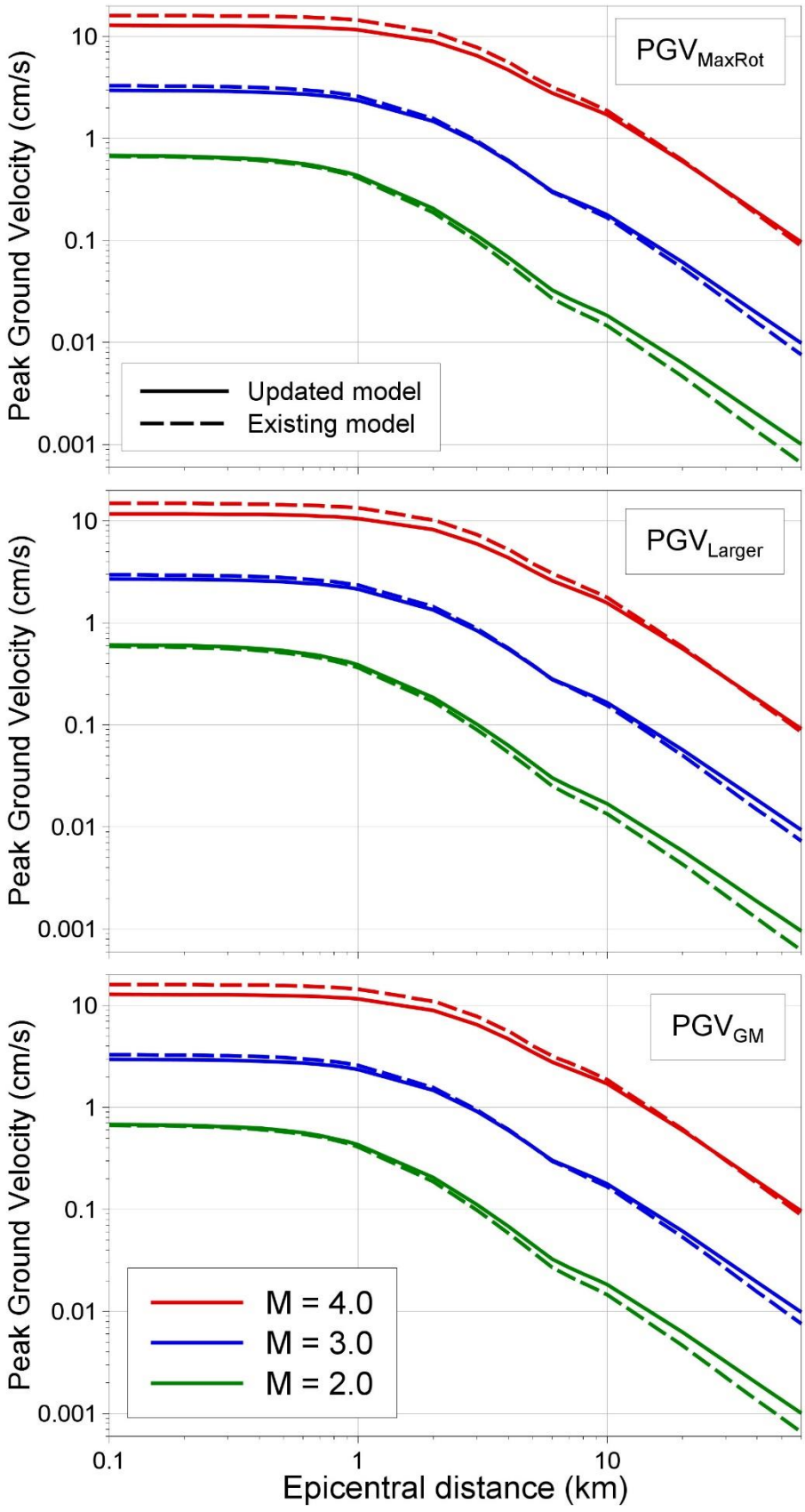

Figure 3.7. Predicted 84-percentile PGV values from the old and new models against distance for magnitudes M_L 2, 3 and 4

4. Concluding Remarks

New empirical PGV equations calibrated to the Groningen field have been derived, using three different definitions of the horizontal component of motion: the geometric mean of the two horizontal components, the larger of the two horizontal components, and the maximum component identified by rotation of the recorded traces. These models are applicable for earthquakes with magnitudes between M_L 1.8 and M_L 3.6 and at epicentral distances of up to about 35 km. A small extrapolation to larger distances, perhaps to about 50 km, can be made with reasonable confidence but the equation should not be applied outside the Groningen field. Extrapolation to smaller or larger magnitudes is not advisable.

These new equations are an update of those issued one year ago (Bommer *et al.*, 2017c). The update has been made because of a large number of additional records have become available and also KNMI has made some corrections to the surface accelerographs of the G-network. The most notable changes to the model from the previous version are a decrease in the strength of the magnitude scaling and a very notable reduction in the between-earthquake variability, which leads to a modest reduction of the overall sigma. The new model predicts slightly larger median PGV values in the magnitude range of the data than the previous model, with these differences becoming larger at greater distance. For an earthquake of M_L 2, the updated median predictions are about 10% larger at short distance, increasing to 27% larger at 5 km, 35% larger at 10 km, and 45% larger at 20 km. The differences reduce with increasing magnitude such that even at M_L 2.5, there is just under a 25% increase at 10 km.

5. References

Bommer, J.J., P.J. Stafford, B. Edwards, B. Dost, E. van Dedem, A. Rodriguez-Marek, P. Kruiver, J. van Elk, D. Doornhof & M. Ntinalexis (2017a). Framework for a ground-motion model for induced seismic hazard and risk analysis in the Groningen gas field, The Netherlands. *Earthquake Spectra* **33**(2), 481-498.

Bommer, J.J., B. Dost, B. Edwards, P.P. Kruiver, M. Ntinalexis, A. Rodriguez-Marek, P.J. Stafford & J. van Elk (2017b). Developing a model for the prediction of ground motions due to earthquakes in the Groningen gas field. *Netherlands Journal of Geoscience* **96**(5), s203-s213.

Bommer, J.J., P.J. Stafford & M. Ntinalexis (2017c). *Empirical Ground-Motion Prediction Equations for Peak Ground Velocity from Small-Magnitude Earthquakes in the Groningen Field Using Multiple Definitions of the Horizontal Component of Motion: Updated Model for Application to Smaller Earthquakes.* Report to NAM, 23 November, 14 pp.